Inverse structure problem for neutron-star binaries

Lee Lindblom
Center for Astrophysics and Space Sciences, University of California at San Diego, La Jolla, California 92093, USA

(Received 6 July 2018; published 14 August 2018)

Gravitational wave detectors in the LIGO/Virgo frequency band are able to measure the individual masses and the composite tidal deformabilities of neutron-star binary systems. This paper demonstrates that high accuracy measurements of these quantities from an ensemble of binary systems can in principle be used to determine the high density neutron-star equation of state exactly. This analysis assumes that all neutron stars have the same thermodynamically stable equation of state, but does not use simplifying approximations for the composite tidal deformability or make additional assumptions about the high density equation of state.

DOI: 10.1103/PhysRevD.98.043012

I. INTRODUCTION

The masses, M, and the tidal deformabilities, Λ, of neutron stars can (in principle) be measured by observations of the gravitational waves emitted during the last stages of the inspiral of neutron-star binary systems [1]. Since all neutron stars are expected to have the same equation of state, accurate measurements of M and Λ for an ensemble of neutron stars could be used to determine the high density portion of the neutron star equation of state exactly by solving the inverse stellar structure problem [2–4].

Unfortunately, the individual tidal deformabilities of the stars in a neutron-star binary system are not accurately observable by gravitational wave detectors operating in the LIGO/Virgo frequency band.[1] Instead a composite tidal deformability $\tilde{\Lambda}$, representing the deformability of the binary system as a whole, is observable with such detectors. This composite tidal deformability is related to the properties of the individual stars by

$$\tilde{\Lambda} = \frac{16}{13}\frac{M_1^4(M_1+12M_2)\Lambda_1 + M_2^4(M_2+12M_1)\Lambda_2}{(M_1+M_2)^5}, \quad (1)$$

where Λ_1 and Λ_2 are the tidal deformabilities, and $M_1 \geq M_2$ are the masses of the individual stars [1,5,6]. The observation of gravitational waves from a neutron-star binary, GW170817, provides the first (and at present only) observation of M_1, M_2 and $\tilde{\Lambda}$ for a binary system [7,8].

The purpose of this paper is to explore the extent to which measurements of the masses, M_1 and M_2, and the composite tidal deformabilities, $\tilde{\Lambda}$, of neutron-star binaries can in principle be used to determine the high density portion of the neutron-star equation of state. Could such measurements determine the equation of state exactly (assuming the measurement errors could be made arbitrarily small) through the solution of some appropriate inverse structure problem? Or, are such measurements only able to constrain the equation of state in some way?

An inverse structure problem determines the equation of state of the matter in an astrophysical system using measurements of the macroscopic properties of that system. Mathematically well posed inverse structure problems do exist for individual neutron stars [2–4,9,10]. In particular, given a complete knowledge of the curve of observables, $M(p_c)$ and $\Lambda(p_c)$ (parameterized e.g., by the central pressures p_c of the stars), this curve exactly determines the equation of state, $\epsilon = \epsilon(p)$, a curve in the energy density ϵ, pressure p space. It is not surprising that the stellar structure equations determine this unique relationship (and inverse relationship) between these curves. It is less obvious that an analogous inverse structure problem exists for binary systems. Does a complete knowledge of the two-dimensional surface of observables for binary systems, $M_1(p_{1c})$, $M_2(p_{2c})$ and $\tilde{\Lambda}(p_{1c}, p_{2c})$ (parametrized e.g., by the central pressures, p_{1c} and p_{2c}, of each star) determine the equation of state exactly as well?

The inverse structure problem for neutron-star binaries does have an almost trivial formal solution. Given a complete knowledge of the surface of observables, $\{M_1(p_{1c}), M_2(p_{2c}), \tilde{\Lambda}(p_{1c}, p_{2c})\}$, the equation of state

[1]Tidal distortion effects first appear in the post-Newtonian expansion of the gravitational waveform at order $(v/c)^{10}$ as a term proportional to a composite deformability parameter. It is only at even higher order that additional terms appear that would allow the deformabilities of the individual stars to be determined. Gravitational wave detectors operating in the LIGO/Virgo frequency band are never likely to be able to measure those high order terms in neutron-star binary systems.

can be determined exactly by restricting attention to equal-mass binaries: $M_1(p_{1c}) = M_2(p_{2c})$, so that $p_{1c} = p_{2c}$ and $\Lambda_1(p_{1c}) = \Lambda_2(p_{1c}) = \tilde{\Lambda}(p_{1c}, p_{1c})$. The inverse structure problem for binaries in this special case reduces to the single neutron-star inverse structure problem, and that problem can be solved exactly in various ways [2–4]. Unfortunately, observations of precisely equal mass binary systems will never be available. So, the interesting question is not whether the inverse structure problem for binaries has a formal solution, but rather how (and how well) it can be solved using measurements from a random ensemble of unequal mass binary systems.

The method proposed here for solving the inverse structure problem for binaries is a fairly straightforward generalization of the method developed previously for individual neutron stars [2–4]. Consider a random ensemble of data points, $\{M_{1i}, M_{2i}, \tilde{\Lambda}_i\}$ for $i = 1, \ldots, N_B$, taken from the exact surface of observables. The goal is to find an equation of state whose model observables match these data. This is done by introducing a parametric representation of the equation of state, $\epsilon = \epsilon(p, \gamma_k)$, where the γ_k are parameters whose values can be adjusted to approximate any equation of state to any desired accuracy [11–13]. Given this equation of state model, and choices for the central pressures of each of the stars in the binary, p^i_{1c} and p^i_{2c}, it is straightforward to integrate the stellar structure equations to determine the masses $M_1(p^i_{1c}, \gamma_k)$ and $M_2(p^i_{2c}, \gamma_k)$, and the tidal deformabilities $\Lambda_1(p^i_{1c}, \gamma_k)$ and $\Lambda_2(p^i_{2c}, \gamma_k)$. The resulting model observables $M_1(p^i_{1c}, \gamma_k)$, $M_2(p^i_{2c}, \gamma_k)$ and $\tilde{\Lambda}(p^i_{1c}, p^i_{2c}, \gamma_k)$ from Eq. (1), are then compared to the exact data using the quantity χ^2 that measures the modeling error:

$$\chi^2(p^i_{1c}, p^i_{2c}, \gamma_k) = \frac{1}{N_{\rm B}} \sum_{i=1}^{N_{\rm B}} \left\{ \left[\log\left(\frac{M_1(p^i_{1c}, \gamma_k)}{M_{1i}} \right) \right]^2 + \left[\log\left(\frac{M_2(p^i_{2c}, \gamma_k)}{M_{2i}} \right) \right]^2 + \left[\log\left(\frac{\tilde{\Lambda}(p^i_{1c}, p^i_{2c}, \gamma_k)}{\tilde{\Lambda}_i} \right) \right]^2 \right\}. \tag{2}$$

The error measure, χ^2, is then minimized over the $2N_B + N_\gamma$ dimensional space of parameters $\{p^i_{1c}, p^i_{2c}, \gamma_k\}$. The location of this minimum determines an equation of state model, $\epsilon = \epsilon(p, \gamma_k)$, whose stellar models best fit the observations.

The equation of state, $\epsilon = \epsilon(p, \gamma_k)$, obtained by minimizing χ^2 in Eq. (2) provides an approximation to the physical neutron-star equation of state. If this method of solving the inverse structure problem for binaries is successful, these approximate equations of state should become more accurate as N_γ the number of parameters in the equation of state model, and as N_B the number of binary data points are increased.

The remainder of this paper describes a series of numerical tests that illustrate how well this inversion method actually works in practice. Section II describes the construction of mock data, $\{M_{1i}, M_{2i}, \tilde{\Lambda}_i\}$ for $i = 1, \ldots, N_B$, from a known equation of state. Section III describes the parametric representations of the equation of state used in these tests. These representations, based on spectral expansions of the adiabatic index, are shown to converge exponentially to the "exact" equation of state used for the mock data in Sec. II. Section IV solves the inverse structure problem with these mock binary data using the method described above to determine approximate parametric model equations of state. The accuracy of these model equations of state are then evaluated by comparing them to the original "exact" equation of state used to construct the mock data. These results are described at length in Secs. IV and V. In summary: the errors in the equation of state models decrease exponentially in these tests as the number of parameters N_γ is increased. This method for solving the inverse structure problem for binaries therefore works very well.

II. MOCK BINARY DATA

Gravitational wave observations of neutron-star binaries can measure the masses, M_1 and M_2, and the composite tidal deformabilities $\tilde{\Lambda}$ of those systems. Mock data, $\{M_{1i}, M_{2i}, \tilde{\Lambda}_i\}$ for $i = 1, \ldots, N_B$, are constructed in this section, to be used in Sec. IV to test the solution to the inverse structure problem for binaries outlined in Sec. I. These mock data are constructed from the simple pseudopolytrope,

$$p = p_0 \left(\frac{\epsilon}{\epsilon_0} \right)^2, \tag{3}$$

chosen as the exemplar "exact" equation of state in part because its adiabatic index is similar to more realistic models of neutron-star matter. For these tests the constants p_0 and ϵ_0 are chosen to have the values $p_0 = 8 \times 10^{33}$ and $\epsilon_0 = 2 \times 10^{14}$ in cgs units. The resulting equation of state produces a maximum mass neutron-star model of about $2.339 M_\odot$.

The goal of the numerical tests performed in Sec. IV is to determine how well and how accurately the method for solving the inverse structure problem described in Sec. I actually works. To do this effectively, extremely accurate mock data are needed. The stellar structure equations can be solved numerically more accurately using an enthalpy based rather than the standard pressure based form of those equations [9].[2] Consequently it is useful to re-write the

[2]The enthalpy of the star approaches zero linearly at the surface of the star, while the pressure approaches zero as a relatively high power of the distance from the surface. Consequently it is much more difficult to determine the location of the surface (and the other macroscopic observables of the star) accurately using the standard pressure based forms of the equations.

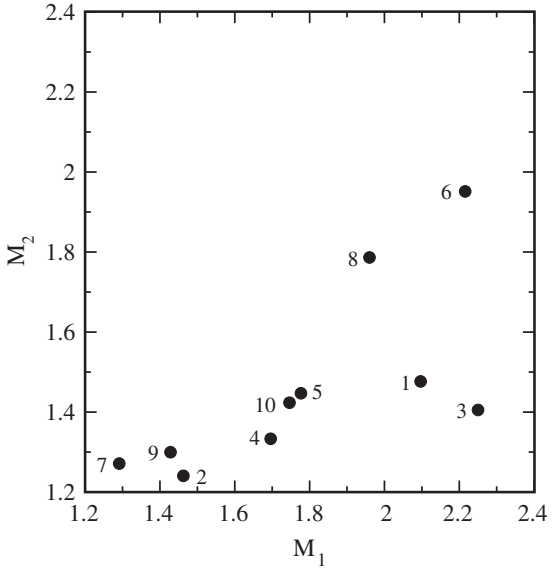

FIG. 1. Points indicate the randomly chosen mass pairs $M_1 \geq M_2$ included in the mock data set.

equation of state in terms of the enthalpy h. The simple equation of state used for these tests, Eq. (3), has the following enthalpy based form,

$$\epsilon(h) = \frac{\epsilon_0^2 c^2}{p_0}(e^{h/2} - 1), \tag{4}$$

$$p(h) = \frac{\epsilon_0^2 c^4}{p_0}(e^{h/2} - 1)^2. \tag{5}$$

The masses M_1 and M_2 in these mock data are computed by solving the standard Oppenheimer-Volkoff equations [14] transformed into enthalpy based forms [9]. And, the tidal deformabilities are computed using the equations derived by Hinderer [5,6], but transformed into enthalpy based forms [2,3]. The central enthalpies, h_{1c}^i and h_{2c}^i, for the stars in each mock binary system are chosen with a random number generator from the range needed to produce stars with masses between $1.2M_\odot$ and the maximum mass $2.339M_\odot$.[3] Figure 1 illustrates the resulting mock binary systems that are used in the numerical tests in Sec. IV. The number labels of the mass-pair points indicate the (randomly chosen) order in which the models are used in the inversion tests. For example, a test involving N_B binaries would use the data points labeled $1, \ldots, N_B$.

[3]The stellar models used for the mock data were constructed in a two step process. First a large collection of $N_{\rm stars}$ models were constructed whose central enthalpies are given by $h_c^n = h_{\rm min} + (h_{\rm max} - h_{\rm min})(n/N_{\rm stars})^2$ for $n = 1, \ldots, N_{\rm stars}$, with $h_{\rm min}$ and $h_{\rm max}$ being the central enthalpies of the models with $M = 1.2M_\odot$ and $M = 2.339M_\odot$ respectively. This choice of the h_c^n produces a collection of stellar models $\{M_n, \Lambda_n\}$ having (roughly) equally spaced masses. The second step uses a random number generator, ran2 from Ref. [15], to generate a uniformly distributed random sequence of integers $1 \leq \ell \leq N_{\rm stars} = 1000$. This random sequence of integers is then used to select the particular stellar models used as the mock data for these tests, $\{M_i, \Lambda_i\}$, from the much larger collection of models $\{M_n, \Lambda_n\}$.

III. PARAMETRIC REPRESENTATIONS OF THE EQUATION OF STATE

This section describes the parametric representations of the equation of state used in the numerical tests of the inverse structure problem in Sec. IV. Since these tests use enthalpy based representations of the stellar structure equations, enthalpy based parametric representations of the equation of state are needed. The most efficient representations of this type presently available are based on spectral representations of the adiabatic index $\Gamma(h)$ [12]. The best studied example uses the expansion,

$$\log\Gamma(h, \gamma_k) = \sum_{k=1}^{N_\gamma} \gamma_k \left[\log\left(\frac{h}{h_0}\right)\right]^{k-1}, \tag{6}$$

where the γ_k are adjustable parameters, and h_0 determines the low density limit of the domain where the spectral representation is to be used. For these tests the constant h_0 is chosen to correspond to a density at the outer boundary of the neutron-star core $\epsilon_0 = \epsilon(h_0) = 2 \times 10^{14}$ g/cm^3. Below this density the equation of state is assumed to be known, and is taken in our tests to be the exact equation of state given in Eqs. (4) and (5). Given this expression for $\Gamma(h, \gamma_k)$, the parametric equation of state itself is determined by the expressions [12]

$$p(h, \gamma_k) = p_0 \exp\left[\int_{h_0}^{h} \frac{e^{h'} dh'}{\mu(h', \gamma_k)}\right], \tag{7}$$

$$\epsilon(h, \gamma_k) = p(h, \gamma_k)\frac{e^h - \mu(h, \gamma_k)}{\mu(h, \gamma_k)}, \tag{8}$$

where $\mu(h, \gamma_k)$ is defined as,

$$\mu(h, \gamma_k) = \frac{p_0 e^{h_0}}{\epsilon_0 + p_0} + \int_{h_0}^{h} \frac{\Gamma(h', \gamma_k) - 1}{\Gamma(h', \gamma_k)} e^{h'} dh'. \tag{9}$$

These parametric equations of states have been used successfully to represent a variety of realistic nuclear-theory model equations of state, with errors that converge toward zero as the number of parameters N_γ is increased [12,13]. These representations are used in Sec. IV as approximations to the "exact" equation of state as determined by the mock binary data from Sec. II. It is useful to understand, therefore, how well these parametric representations are able to represent this "exact" equation of state. The adiabatic index for the "exact" equation of state of Eq. (3) is given by

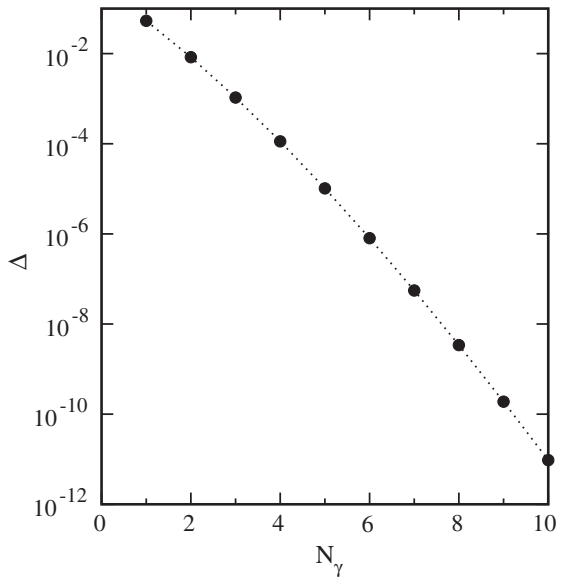

FIG. 2. Points illustrate the average errors Δ of the enthalpy-based spectral representations of the "exact" equation of state as a function of the order of the spectral representation, N_γ.

$$\Gamma(h) = \frac{\epsilon c^2 + p}{p c^2}\frac{dp}{d\epsilon} = 2\frac{\epsilon c^2 + p}{\epsilon c^2} = 2 + 2(1 - e^{h/2})^2. \quad (10)$$

While this $\Gamma(h)$ is quite simple, its representation as the spectral expansion given in Eq. (6) requires an infinite number of terms. The optimal values of the parameters γ_k can be estimated by minimizing the equation of state error measure $\Delta(\gamma_k)$, defined as

$$\Delta^2(\gamma_k) = \frac{1}{N}\sum_{i=1}^{N}\left[\log\left(\frac{\epsilon(h_i,\gamma_k)}{\epsilon_i}\right)\right]^2 \quad (11)$$

with respect to the N_γ spectral parameters γ_k. The sum in this expression is taken over $N \approx 85$ points taken from an exact equation of state table, equally spaced in $\log\epsilon$ in the density range $2\times 10^{14} \le \epsilon_i \le 1.8895\times 10^{15}$ g/cm^3 that covers the high density cores of all neutron stars with this equation of state. This sum measures the differences between the parametric equation of state densities $\epsilon(h_i,\gamma_k)$ with N exact densities $\epsilon_i = \epsilon(h_i)$. Figure 2 shows the minimum values of Δ as a function of the number of spectral parameters N_γ. These parametric representations therefore converge exponentially toward Eq. (3), and Fig. 2 provides a best-case estimate of the accuracy that the approximate solutions to the inverse problem in Sec. IV might achieve.

Based on our understanding of other spectral representations, like Fourier series, the spectral parametric representations used here are expected to converge exponentially for all smooth equations of state. The rate of exponential convergence will depend, however, on the detailed structure of the particular equation of state. Equations of state having more "structure" than the simple pseudopolytrope studied here will converge more slowly. Spectral parametric representations of equations of state having phase transitions (i.e., discontinuities in the equation of state or its derivatives) are also expected to converge, however the rate of convergence in those cases are expected to be polynomial rather than exponential.

IV. NUMERICAL INVERSION TESTS

The goal of the inverse structure problem for binaries is to determine the equation of state from a knowledge of the observables $\{M_1(h_{1c}), M_2(h_{2c}), \tilde{\Lambda}(h_{1c}, h_{2c})\}$ (parametrized here by the central enthalpies h_{1c} and h_{2c} of each star). Let $\{M_{1i}, M_{2i}, \tilde{\Lambda}_i\}$ for $i = 1, \ldots, N_B$ denote a random ensemble of points from the exact surface of observables, and let $\epsilon = \epsilon(h,\gamma_k)$ and $p = p(h,\gamma_k)$ denote a family of parametric equations of state. The proposal is to construct approximate solutions to this inverse structure problem by minimizing the difference between models of the observables $\{M_1(h_{1c},\gamma_k), M_2(h_{2c},\gamma_k), \tilde{\Lambda}(h_{1c},h_{2c},\gamma_k)\}$ based on the parametric equation of state, and the observational data points $\{M_{1i}, M_{2i}, \tilde{\Lambda}_i\}$. This difference is measured using the modeling error measure $\chi^2(h^i_{1c}, h^i_{2c}, \gamma_k)$, defined by

$$\chi^2(h^i_{1c}, h^i_{2c}, \gamma_k) = \frac{1}{N_B}\sum_{i=1}^{N_B}\left\{\left[\log\left(\frac{M_1(h^i_{1c},\gamma_k)}{M_{1i}}\right)\right]^2 + \left[\log\left(\frac{M_2(h^i_{2c},\gamma_k)}{M_{2i}}\right)\right]^2 + \left[\log\left(\frac{\tilde{\Lambda}(h^i_{1c},h^i_{2c},\gamma_k)}{\tilde{\Lambda}_i}\right)\right]^2\right\}. \quad (12)$$

The best-fit model is identified by minimizing the modeling error $\chi^2(h^i_{1c}, h^i_{2c}, \gamma_k)$ with respect to the $2N_B + N_\gamma$ parameters $\{h^i_{1c}, h^i_{2c}, \gamma_k\}$. The parametric equation of state $\epsilon = \epsilon(h,\gamma_k)$ and $p = p(h,\gamma_k)$ with γ_k evaluated at this minimum is an approximate solution to the inverse structure problem.

The most difficult step in this approach is finding the minimum of $\chi^2(h^i_{1c}, h^i_{2c}, \gamma_k)$ numerically. The minimization method used for these tests is the Levenberg-Marquardt algorithm [15]. This is a steepest descent type algorithm that requires as input the value of the function, $\chi^2(h^i_{1c}, h^i_{2c}, \gamma_k)$, and its partial derivatives with respect to each of the parameters. The needed partial derivatives can be constructed from $\partial M/\partial h_c$, $\partial\Lambda/\partial h_c$, $\partial M/\partial\gamma_k$ and $\partial\Lambda/\partial\gamma_k$ (computed for these tests using the methods described in Refs. [2,3]) plus the derivatives

$$\frac{\partial\tilde{\Lambda}}{\partial M_1} = -\frac{16M_1^3M_2(7M_1 - 48M_2)\Lambda_1}{13(M_1+M_2)^6} - \frac{16M_2^4(48M_1 - 7M_2)\Lambda_2}{13(M_1+M_2)^6}, \quad (13)$$

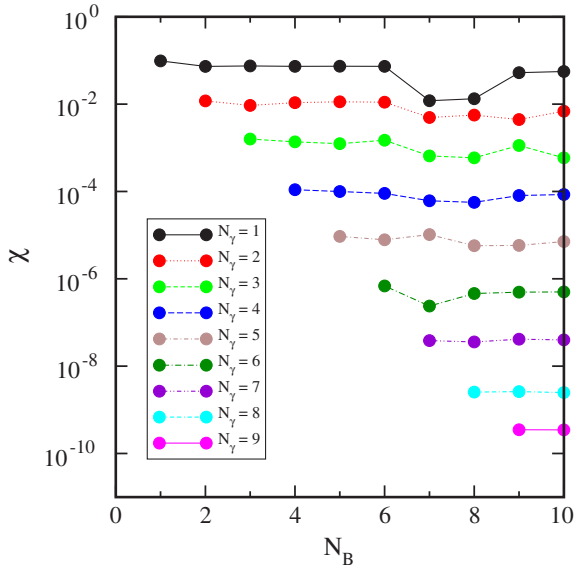

FIG. 3. Curves indicate the minimum values of $\chi(h^i_{1c}, h^i_{2c}, \gamma_k)$ achieved for different numbers N_γ of spectral parameters, and different numbers N_B of mock binary data points.

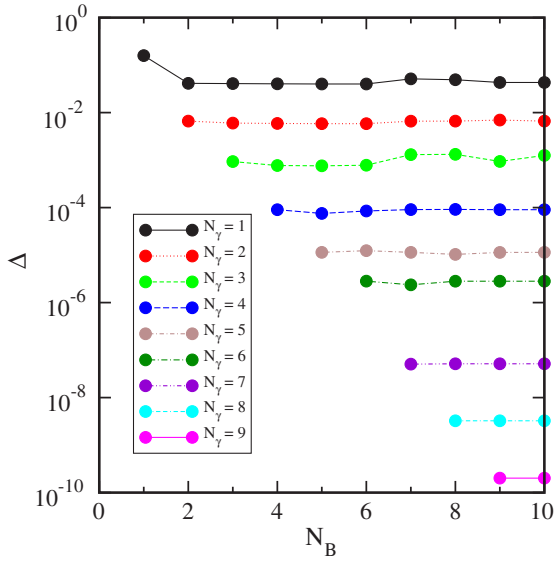

FIG. 4. Curves indicate the values of $\Delta(\gamma_k)$ for the γ_k that minimize $\chi(h^i_{1c}, h^i_{2c}, \gamma_k)$ for different numbers N_γ of spectral parameters, and different numbers N_B of mock binary data points.

$$\frac{\partial\tilde{\Lambda}}{\partial M_2}=\frac{16M_1^4(7M_1-48M_2)\Lambda_1}{13(M_1+M_2)^6}+\frac{16M_1M_2^3(48M_1-7M_2)\Lambda_2}{13(M_1+M_2)^6}, \tag{14}$$

$$\frac{\partial\tilde{\Lambda}}{\partial\Lambda_1}=\frac{16M_1^4(M_1+12M_2)}{13(M_1+M_2)^5}, \tag{15}$$

$$\frac{\partial\tilde{\Lambda}}{\partial\Lambda_2}=\frac{16M_2^4(M_2+12M_1)}{13(M_1+M_2)^5}. \tag{16}$$

The Levenberg-Marquardt minimization method is very fast and very accurate at locating the local minimum close to any given initial parameter point. It often fails to find the smallest minimum, however, if the function has many local minima. To avoid unwanted local minima, and to speed up the calculation, the numerical minimizations performed for these tests were initialized using the exact values of the parameters h^i_{1c} and h^i_{2c} from Sec. II, and the best-fit values of the parameters γ_k described in Sec. III. The minimization procedure is iterated as many times as needed (typically less than ten) until χ is unchanged from one step to the next.[4]

Figure 3 illustrates the minimum values of χ obtained in this way for different values of N_γ and N_B. The equations used to locate the minimum of χ are degenerate whenever the number of parameters, $2N_B + N_\gamma$, is less than the number of data points, $3N_B$. Consequently these minima were only computed for $N_\gamma \leq N_B$. This figure shows that the numerically determined values of the minima of χ decrease exponentially as the number of equation of state parameters N_γ is increased. These minima are relatively insensitive to the values of N_B for fixed values of N_γ.

Figure 4 shows the accuracy of the parametric equations of state whose spectral parameters γ_k are set by the minima of χ shown in Fig. 3. These equation of state errors are measured with the quantity Δ defined in Eq. (11). Like the observational data modeling errors χ, the equation of state errors Δ decrease exponentially as N_γ is increased, but are relatively insensitive to N_B for fixed N_γ.[5]

Figures 3 and 4 show that the modeling errors $\chi(N_\gamma)$ are comparable to the equation of state modeling errors $\Delta(N_\gamma)$ for the simple mock data used in these tests. This rough comparability of these errors is expected to apply even for more complicated, more realistic equations of state. Since representations of more realistic equations of state are expected to converge more slowly, the modeling errors χ are also expected to converge more slowly in those cases. For smooth equations of state, these convergence rates are expected to be exponential in the number of parameters N_γ. Equations of state having phase transitions are expected to converge as a power of N_γ, with a power that depends on the order of the phase transition.

[4]In the analysis of real neutron-star observations, it will not be possible to know *a priori* what the optimal parameters h^i_{1c}, h^i_{2c} and γ_k are likely to be. In this case it will almost certainly be necessary to adopt more powerful computational methods for locating the absolute minimum of the complicated nonlinear function $\chi^2(h^i_{1c}, h^i_{2c}, \gamma_k)$.

[5]The results for $N_\gamma = 10$ are not shown in Figs. 3 and 4, because the rates of convergence decreased abruptly at this point. This is probably caused by numerical inaccuracies at the 10^{-10}–10^{-11} level in some part of the code. Since the source of those errors was not identified, and since the results for $N_\gamma = 10$ appeared to be unreliable, they were not displayed with the $N_\gamma < 10$ results.

V. DISCUSSION

The results of the numerical tests in Sec. IV confirm that the method of solving the inverse structure problem for neutron-star binaries outlined in Sec. I is mathematically convergent using data from a randomly chosen ensemble of binaries. The equation of state accuracies shown in Fig. 4 are comparable to the best-fit errors for this equation of state in Fig. 2. So this method of determining the equation of state is also very efficient.

Important features of the analysis presented here are its generality and lack of simplifying assumptions. No assumptions are made about the equation of state in the cores of neutron stars other than thermodynamic stability. Thermodynamic stability requires the equation of state function $\epsilon(p)$ to be monotonically increasing. It is imposed implicitly by the spectral expansion for the adiabatic index $\Gamma(h)$ in Eq. (6) that ensures $\Gamma(h) \geq 0$. The analysis here also makes no simplifying assumptions about the composite deformabilities $\tilde{\Lambda}$ of the binaries. In contrast, the recent analysis of GW170817 in Ref. [16] assumes the tidal deformabilities of the two neutron stars are related by $\Lambda_1 M_1^6 = \Lambda_2 M_2^6$, while the analysis in Ref. [17] assumes $\Lambda_2 - \Lambda_1$ is a prescribed function of $\Lambda_1 + \Lambda_2$ and the mass ratio M_2/M_1. The analysis here simply evaluates $\tilde{\Lambda}$ exactly using Eq. (1) in terms of the parametric equation of state and the central enthalpies of each star. No additional assumption about the form of $\tilde{\Lambda}$ is needed.

The method proposed here for solving the inverse structure problem for binaries is well posed and admits an exact solution when the number of data points N_B is greater than or equal to the number of equation of state parameters N_γ. In contrast, the recent analyses in Refs. [16–18] attempt to determine four equation of state parameters using Bayesian statistical methods from the observation of the single neutron-star binary GW170817. From the perspective of the exact problem, it is not possible to determine more than one equation of state parameter from the observation of a single binary. Analyzing a single binary using a four parameter equation of state model in the exact case could only restrict the four-dimensional parameter space to some three-dimensional subspace. To make the problem well posed, prior constraints on the equation of state parameters would be needed to fix a particular point on that three-dimensional parameter subspace. In the method proposed here for solving the inverse structure problem, the appropriate dimensional space of parameters is chosen from the beginning by requiring $N_\gamma \leq N_B$. No additional assumptions or prior constraints on the equation of state parameters are needed.

The "exact" equation of state used to create the mock data in these tests is very simple and very smooth. Consequently the rate of convergence of the errors in these tests is probably faster than it would be for more realistic equations of state. The inverse structure problem for single neutron stars [2,3] has been studied using a number of more realistic nuclear-theory model equations of state. The convergence rates for the equation of state errors found here are only a bit faster than those found previously for the smoothest and simplest realistic nuclear-theory based equation of state models (e.g., PAL6). Consequently, the expectation is that the equation of state errors for the binary problem will be similar to those for the single neutron-star inverse problem studied previously. A fairly small number of high accuracy measurements from binary systems should therefore be sufficient to determine the high density neutron-star equation of state at the fraction of a percent level, if such high accuracy measurements ever became available.

The mock data used in the analysis in Sec. IV were constructed with high precision to allow the mathematical convergence tests of the method to be confirmed with high confidence. Those convergence tests were the primary purpose of this paper. Observations from real binary systems will contain significant measurement errors, and those measurement errors will also contribute to the errors in the equations of state determined in this way. More realistic estimates of the equation of state errors achievable by these methods can only be found therefore using more realistic mock data for these tests. The plan for a future study is to introduce random errors into the mock data with a sequence of different sizes, e.g., 1%, 2%, 5%, 10%, 20%, 50% errors, and then to determine how these data errors affect the inferred equation of state errors.

ACKNOWLEDGMENTS

I thank John Friedman and Massimo Tinto for helpful comments and suggestions on a draft manuscript of this paper. This research was supported in part by NSF Grants No. PHY-1604244 and No. DMS-1620366.

[1] E. Flanagan and T. Hinderer, Phys. Rev. D **77**, 021502 (2008).
[2] L. Lindblom and N. M. Indik, Phys. Rev. D **89**, 064003 (2014).
[3] L. Lindblom and N. M. Indik, Phys. Rev. D **93**, 129903 (2016).
[4] L. Lindblom, AIP Conf. Proc. **1577**, 153 (2014).
[5] T. Hinderer, Astrophys. J. **677**, 1216 (2008).
[6] T. Hinderer, Astrophys. J. **697**, 964 (2009).
[7] B. P. Abbott *et al.* (LIGO Scientific Collaboration and Virgo Collaboration), Phys. Rev. Lett. **119**, 161101 (2017).

[8] B. P. Abbott *et al.* (LIGO Scientific Collaboration and Virgo Collaboration), arXiv:1805.11579.
[9] L. Lindblom, Astrophys. J. **398**, 569 (1992).
[10] L. Lindblom and N. M. Indik, Phys. Rev. D **86**, 084003 (2012).
[11] J. S. Read, B. D. Lackey, B. J. Owen, and J. L. Friedman, Phys. Rev. D **79**, 124032 (2009).
[12] L. Lindblom, Phys. Rev. D **82**, 103011 (2010).
[13] L. Lindblom, Phys. Rev. D **97**, 123019 (2018).
[14] J. R. Oppenheimer and G. M. Volkoff, Phys. Rev. **55**, 374 (1939).
[15] W. H. Press, S. A. Teukolsky, W. T. Vetterling, and B. P. Flannery, *Numerical Recipes in FORTRAN*, 2nd ed. (Cambridge University Press, Cambridge, England, 1992).
[16] S. De, D. Finstad, J. M. Lattimer, D. A. Brown, E. Berger, and C. M. Biwer (2018), arXiv:1804.08583.
[17] B. P. Abbott *et al.* (LIGO Scientific Collaboration and Virgo Collaboration), arXiv:1805.11581.
[18] M. F. Carney, L. E. Wade, and B. S. Irwin, arXiv:1805.11217.